

TONE MAGISTER, Ph.D.
 E-mail: tone.magister@fpp.edu
 University of Ljubljana,
 Faculty of Maritime Studies and Transport
 Unmanned Transport Systems Laboratory
 Pot pomorščakov 4, SI-6320 Portorož, Republic of Slovenia

Science in Traffic and Transport
 Original Scientific Paper
 Accepted: June 11, 2008
 Approved: Sep. 16, 2009

LONG RANGE AIRCRAFT TRAJECTORY PREDICTION

ABSTRACT

The subject of the paper is the improvement of the aircraft future trajectory prediction accuracy for long-range airborne separation assurance. The strategic planning of safe aircraft flights and effective conflict avoidance tactics demand timely and accurate conflict detection based upon future four-dimensional airborne traffic situation prediction which is as accurate as each aircraft flight trajectory prediction. The improved kinematics model of aircraft relative flight considering flight crew intention, aircraft true airspeed variability, and atmosphere conditions is introduced in the paper. The study is focused on improved kinematics model of aircraft relative flight position error estimation. Operational airborne separation capabilities are outlined based on the comparison between the improved and simple model of aircraft relative flight.

KEY WORDS

aircraft trajectory prediction, trajectory prediction error, aircraft position prediction error, flight safety

1. INTRODUCTION

To cope with the increasing demand in the crowded skies above and to make unmanned aircraft systems integrated flight operations possible diverse concepts of airspace organization and management are envisioned. The deciding factor for the autonomous-flight [8], free-flight [5], sector-less [1], and automated [3] airspace feasibility is the ability of the future Airborne Separation Assurance Systems (ASAS) onboard each aircraft airborne to correctly and timely detect every potential in-flight conflict of lost separation. However, the conflict can only be detected opportunely and accurately if the ASAS is based upon four-dimensional prediction of airborne traffic situation. The stability of the latter depends crucially upon the future trajectory of each and every aircraft aloft prediction accuracy.

The problem is that with the existing technology and methodology the look-ahead time for the construction of accurate future trajectory of aircraft flight is reduced to only about 5 to 7 minutes in advance [6]. The longer look-ahead time results in predicted traffic

situation instability [5] and consequently unreliability or even inability of conflict detection.

A simple Traffic Collision Avoidance System-like model of flight predicts each aircraft future trajectory with extrapolation of its ground speed vector from the aircraft last position, while the aircraft ground speed vector is derived with interpolation between its last two known positions. For two aircraft encounters the simple model [9], where an aircraft about to descent and the intruder are denoted by index 2 and 1 respectively, can be written as:

$$\begin{aligned} x_R &= v_{2G} \cos \psi_R - v_{1G} \\ y_R &= v_{2G} \sin \psi_R \\ z_R &= -v_{2G} \tan \theta_R \end{aligned} \quad (1)$$

Obviously, this model (1) is based upon the presumptions of: (a) constant aircraft ground speed and direction v_G , resulting in constant relative angles between aircraft in the horizontal ψ_R and vertical θ_R plane, and therefore including (b) constant wind speed and direction, and (c) constant static state (temperature) of atmosphere as well. Impaired by the uncertainty in future aircraft trajectory, the simple model of aircraft relative flight (1) can be regarded as a short-range conflict detection instrument since it cannot account for the flight crew future intent regarding aircraft trajectory and flight regime as well as for weather conditions and future aircraft trajectory variations due to the aircraft true airspeed variability. The longer look-ahead time based on the simple model of flight decreases the trajectory prediction accuracy which increases the air traffic controller safety margins as they are formed through experience and reflect the biasing of decisions to favour safety over accuracy including expectations regarding uncertainty in aircraft trajectory [7] reducing in the process the airspace utilization as well as air traffic flow efficiency.

Because of the problem described, the ASAS on-board aircraft cannot assure conflict-free trajectory generation for descent through the autonomous flight airspace (AFA) as envisioned in [8] where probabilities of in-flight conflicts are dispersed along the descent trajectory with progressively dictated parameters of flight along the transitioning route before aircraft leaves the AFA. Furthermore, because of the

conflict detection inaccuracies and uncertainties, the conflict- (traffic-) free transition corridor between the AFA and non-AFA airspace cannot be selected, found or predicted as the meta-level control based on reinforcement-learning algorithms decision support [11] might be regarded as an essential prerequisite. One of the possible real world examples for the problems described is the unmanned aircraft system operating as pseudo-satellite at flight levels 500-600 descending after a prolonged mission. Another application of solution to the problems described is aircraft trajectory protection when the responsibilities of the hijacked aircraft crew are transferred to the automatic emergency landing (return) system.

2. AIRCRAFT RELATIVE FLIGHT MODEL

For enhanced forecast of future four-dimensional airborne traffic situation stability under longer look-ahead times and improved conflict detection accuracy and reliability, the improved kinematics model of aircraft relative flight was derived to include not only for the aircraft crew future intent as introduced in [6] but to consider:

- a) the aircraft true airspeed v variableness $v = v(\vartheta_S(z))$ as a function of a static state of an atmosphere ϑ_S (i. e. the static air temperature T ; $\vartheta_S(z) = \{T(z)\}$) variation with aircraft pressure altitude z ,
- b) the aircraft true airspeed variableness $v = v(\sigma(z))$ due to the changing set of speed regimes $\sigma(z) = \{M, v_C\}$ of descent and/or climb with a constant Mach number M and/or with a constant calibrated airspeed v_C ,
- c) an influence of the dynamic state of an atmosphere $\vartheta_D(z) = \{w(z), \xi(z)\}$ defined with the wind speed w and direction ξ on the progressive speed V of an aircraft which can be written as $V = V(v, \vartheta_D(z))$.

It is envisioned that the ASAS on-board aircraft are communicating via airborne dependant surveillance-broadcast (ADS-B) system and the future traffic situation is based upon the negotiation about future trajectories between aircraft allowing them to benefit from multiple independent declarative analysis of the same situation [10].

Based on the simplification that an angular velocity vector of each aircraft equals zero, and an assumption that an alteration of each aircraft trajectory is instantaneous (discussed in chapter §3.1), the advanced model of aircraft relative motion is defined by:

$$\begin{aligned} x'_R &= V_2(v_2(\sigma_2(z), \vartheta_S(z)), \vartheta_D(z)) \cos \theta_R(\sigma_2(z)) \cdot \\ &\quad \cdot \cos \psi_R - V_1(v_1(\sigma_1(z), \vartheta_S(z)), \vartheta_D(z)) \\ y'_R &= V_2(v_2(\sigma_2(z), \vartheta_S(z)), \vartheta_D(z)) \cdot \end{aligned} \quad (2)$$

$$\begin{aligned} &\quad \cdot \sin \theta_R(\sigma_2(z)) \cos \psi_R \\ z'_R &= V_2(v_2(\sigma_2(z), \vartheta_S(z)), \vartheta_D(z)) \sin \theta_R(\sigma_2(z)) \end{aligned}$$

The model of aircraft relative motion (2) can be transformed into a time-dependant function using the rate of climb (+) or descent (-) definition:

$$\pm \frac{dz}{dt} = V(z) \sin \theta_R(\sigma_2(z)) \quad (3)$$

where the progressive speed V of an aircraft follows the form the aircraft speed vector triangle:

$$\begin{aligned} V(z) &= \frac{w \cos(\xi - \psi)}{\cos \theta_R(\sigma_2(z))} + \\ &\quad + \frac{\sqrt{v^2(\sigma(z), \theta_S(z)) - w^2 \sin^2(\xi - \psi)}}{\cos \theta_R(\sigma_2(z))} \end{aligned} \quad (4)$$

The improved model of aircraft relative flight following from (2) is designed from the start to be verifiable as an ASAS component for its safety of operation as defined in [2].

The solution of the kinematic model of aircraft relative flight (2) is presented for the case that aircraft denoted as A2 and its flight parameters denoted by index 2 start its descent from cruise level z_{FL2} in stratosphere $z_{FL2} > z_{tp}$ (tropopause at z_{tp}) at $t_{TOD} > t_0$ after conflict is detected at t_0 , while the intruder denoted by index 1 continues its constant Mach number M level cruise. The airspeed regimes of flight phases of the descending aircraft A2 (denoted by index 2) are scheduled as in [4]. The solution of (2) provided is partitioned according to the descending aircraft flight phases; note that s , c and t denote trigonometric functions of sine, cosine and tangent.

- a) $t_0 \leq t \leq t_{TOD}$ ($t_0 = 0$): the A2 is in a $M_2 = const$ level cruise ($\theta_2 = 0$) in the stratosphere:

$$\begin{aligned} x_R(t) &= X_R(t_0) + \left(w(c_{\lambda_2} c_{\psi_R} - c_{\lambda_1}) - \right. \\ &\quad \left. - \sqrt{M_1^2 a_{FL1}^2 - w^2 s_{\lambda_1}^2} + c_{\psi_R} \sqrt{M_2^2 a_{tp}^2 - w^2 s_{\lambda_2}^2} \right) t \\ y_R(t) &= y_R(t_0) + s_{\psi_R} \left(w c_{\lambda_2} + \sqrt{M_2^2 a_{tp}^2 - w^2 s_{\lambda_2}^2} \right) t \quad (5) \\ z_R(t) &= z_R(t_0) \end{aligned}$$

where $r_R(t_0) = (x_R(t_0), y_R(t_0), z_R(t_0))$ is the initial aircraft relative position when conflict is detected at t_0 .

- b) $t_{TOD} < t \leq t_{ip}$: A2 descends in a constant M speed-regime with a constant angle of descent $\theta_R = \theta_2$ through the stratosphere:

$$\begin{aligned} x_R(t) &= X_R(t_{TOD}) + \left(w(c_{\lambda_2} c_{\psi_R} - c_{\lambda_1}) - \right. \\ &\quad \left. - \sqrt{M_1^2 a_{FL1}^2 - w^2 s_{\lambda_1}^2} + c_{\psi_R} \sqrt{M_2^2 a_{tp}^2 - w^2 s_{\lambda_2}^2} \right) t \\ y_R(t) &= y_R(t_{TOD}) + \\ &\quad + s_{\psi_R} \left(w c_{\lambda_2} + \sqrt{M_2^2 a_{tp}^2 - w^2 s_{\lambda_2}^2} \right) t \quad (6) \\ z_R(t) &= z_R(t_{TOD}) + t \theta_2 \left(w c_{\lambda_2} + \sqrt{M_2^2 a_{tp}^2 - w^2 s_{\lambda_2}^2} \right) t \end{aligned}$$

where $r_R(t_{TOD})$ is a solution of (5) for $t = t_{TOD}$.

- c) $t_{ip} < t \leq t_p$: after passing the tropopause at t_{ip} the A2 descends in a constant M speed-regime through the troposphere:

$$\begin{aligned} x_R(t) &= x_R(t_{ip}) + \left[w(c_{\lambda_2} c_{\psi_R} - c_{\lambda_1}) + \right. \\ &\quad \left. + c_{\psi_R} k_5 M_2 \sqrt{\chi R} - \sqrt{M_1^2 a_{FL}^2 - w^2 s_{\lambda_1}^2} \right] (t - t_{ip}) + \\ &\quad + c_{\psi_R} k_6 M_2 \sqrt{\chi R} (t^2 - t_{ip}^2) \\ y_R(t) &= y_R(t_{ip}) + s_{\psi_R} (t - t_{ip}) (w c_{\lambda_2} + k_5 M_2 \sqrt{\chi R} + \\ &\quad + s_{\psi_R} k_6 M_2 \sqrt{\chi R} (t^2 - t_{ip}^2)) \quad (7) \\ z_R(t) &= z_R(t_{ip}) - t_{\theta_2} (t - t_{ip}) (w c_{\lambda_2} + k_5 M_2 \sqrt{\chi R} + \\ &\quad - t_{\theta_2} k_6 M_2 \sqrt{\chi R} (t^2 - t_{ip}^2)) \end{aligned}$$

where $r_R(t_{ip})$ is a solution of (6) for $t = t_{ip}$, while k_5, k_6 , and k_1 and k_2 are:

$$k_5 = \sqrt{T_{0R} + \frac{L}{2k_2} \left[k_1 - \sqrt{k_1^2 + 4k_2(t_{ip} t_{\theta_2} + z_{ip}(k_1 + k_2 z_{ip}))} \right] - \frac{w^2 s_{\lambda_2}^2}{M_2^2 \chi R}} \quad (8)$$

$$k_6 = L t_{\theta_2} \left(4k_5 \sqrt{k_1^2 + 4k_2(t_{ip} t_{\theta_2} + z_{ip}(k_1 + k_2 z_{ip}))} \right)^{-1} \quad (9)$$

$$k_1 = \left(w c_{\lambda} + \sqrt{M^2 \chi R T_{0R} - w^2 s_{\lambda}^2} \right)^{-1} \quad (10)$$

$$k_2 = \frac{k_1^2 M L \sqrt{\chi R}}{4} \left(T_{0R} - \frac{w^2 s_{\lambda}^2}{M^2 \chi R} \right)^{-\frac{1}{2}} \quad (11)$$

- d) $t > t_p$: at t_p A2 changes its speed-regime and continues its descent through the troposphere with the constant calibrated airspeed ($v_{C2} = const$):

$$\begin{aligned} x_R(t) &= x_R(t_p) + \left[w(c_{\lambda_2} c_{\psi_R} - c_{\lambda_1}) + c_{\psi_R} k_7 - \right. \\ &\quad \left. - \sqrt{M_1^2 a_{FL}^2 - w^2 s_{\lambda_1}^2} \right] (t - t_p) + c_{\psi_R} k_8 (t^2 - t_p^2) \\ y_R(t) &= y_R(t_p) + s_{\psi_R} (t - t_p) (w c_{\lambda_2} + k_7) + \\ &\quad + s_{\psi_R} k_8 (t^2 - t_p^2) \quad (12) \\ z_R(t) &= z_R(t_p) - t_{\theta_2} (t - t_p) (w c_{\lambda_2} + k_7) - \\ &\quad - t_{\theta_2} k_8 (t^2 - t_p^2), \end{aligned}$$

where $r_R(t_p)$ is a solution of (7) for $t = t_p$, while k_7, k_8, k_9, k_{10} , and k_3, k_4 are:

$$k_7 = \sqrt{\frac{2\chi R T_{0R}}{\chi - 1} \left(1 + \frac{L k_9}{2k_4 T_{0R}} \right) \left[k_{10} \left(1 + \frac{L k_9}{2k_4 T_{0R}} \right)^{-\frac{g_0}{LR}} + 1 \right]^{\frac{\chi - 1}{\chi}} - 1} - w^2 s_{\lambda_2}^2 \quad (13)$$

$$\begin{aligned} k_8 &= \frac{\chi R L t_{\theta_2}}{2(\chi - 1)(k_3 - k_9) k_7} \cdot \\ &\quad \left[-1 + \left(k_{10} \left(1 + \frac{L k_9}{2k_4 T_{0R}} \right)^{-\frac{g_0}{LR}} + 1 \right)^{\frac{\chi - 1}{\chi}} \left(1 - \frac{(\chi - 1) g_0 k_{10}}{\chi R L} \left(k_{10} + \left(1 + \frac{L k_9}{2k_4 T_{0R}} \right)^{\frac{g_0}{LR}} \right)^{-1} \right) \right] \quad (14) \end{aligned}$$

$$k_9 = k_3 - \sqrt{k_3^2 + 4k_4(t_{\theta_2} t_p + z_p(k_3 + k_4 z_p))} \quad (15)$$

$$k_{10} = \left(1 + \frac{\chi - 1}{2} \left(\frac{v_{C2}}{a_0} \right)^2 \right)^{\frac{\chi}{\chi - 1}} - 1 \quad (16)$$

$$k_3 = \left(w c_{\lambda} + \sqrt{\frac{v_C^2 T_{0R}}{T_0} - w^2 s_{\lambda}^2} \right)^{-1} \quad (17)$$

$$\begin{aligned} k_4 &= \frac{k_3^2}{4} \left(\frac{v_C^2 T_{0R}}{T_0} - w^2 s_{\lambda}^2 \right)^{\frac{1}{2}} \cdot \\ &\quad \left(\frac{v_C^2 L}{T_0} - 2g_0 \left(1 + \frac{\chi - 1}{2} \left(\frac{v_C}{a_0} \right)^2 \right) \left[1 - \left(1 + \frac{\chi - 1}{2} \left(\frac{v_C}{a_0} \right)^2 \right)^{-\frac{\chi}{\chi - 1}} \right] \right) \quad (18) \end{aligned}$$

The symbols not accounted for in the text are: g_0 - acceleration of gravity, L - (temperature atmospheric) lapse rate, R - universal gas constant, χ - ratio of specific heats, a_0 and a_{FL} - speed of sound at reference level of standard atmosphere and at aircraft flight level (FL), T_0 and T_{0R} - reference SATs of standard and real atmosphere, λ represents the difference between the wind direction ξ and aircraft true heading ψ , while index R denotes the relative parameter.

3. AIRCRAFT TRAJECTORY PREDICTION ERROR

3.1 Theoretical position prediction errors

At the top of descent (TOD) an aircraft starts its rotation $\Omega(t) = (0, \omega_{\theta}, 0)$ (for $t \in [0, t_t]$) about the lateral axis until angle of descent θ is established after transition time t_t as shown in Figure 1.

For the simplicity of the improved model of aircraft relative flight (2) the instantaneous aircraft transition into descent is assumed:

$$\lim_{t_t \rightarrow 0} \frac{V}{\omega_{\theta}} (1 - \cos(\omega_{\theta} t_t)) = 0 \quad (19)$$

$$\lim_{t_t \rightarrow 0} \frac{V}{\omega_{\theta}} \sin(\omega_{\theta} t_t) = 0$$

Because of simplification (19) the aircraft trajectory is not smooth at the TOD resulting in horizontal e_{x-y} and vertical e_z plane error of aircraft position prediction in the period of transition time $t \in [0, t_t]$, and can be theoretically estimated from Figure 1 as:

$$e_{x-y}(t_t) = V(t_t) \left(\cos \theta - \frac{\sin \theta}{\theta} \right) t_t \quad (20)$$

$$e_z(t_t) = V(t_t) \left(\sin \theta - \frac{1 - \cos \theta}{\theta} \right) t_t$$

The position errors e_{x-y} and e_z (20) are proportional to the transition time t_t , angle of descent θ , and aircraft progressive speed $V = f(v(\sigma(z), \vartheta_S(z)), \vartheta_D)$. They reach their maximum after transition into de-

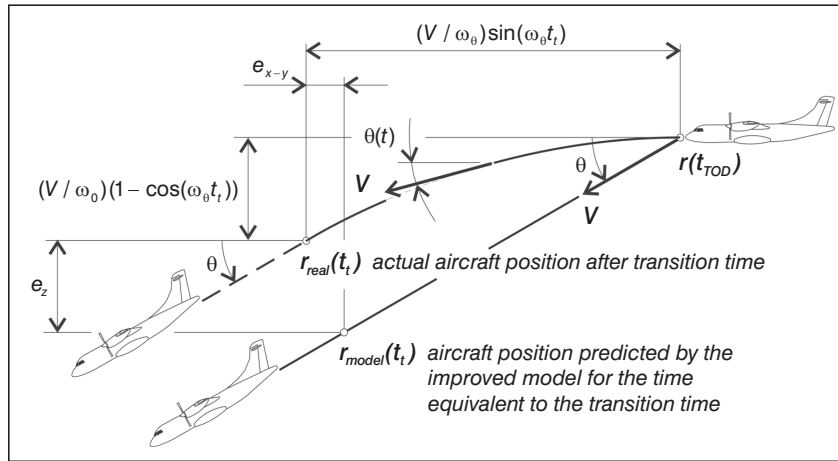


Figure 1 – Simplified transition into descent

scend is completed at t_t ; however, after transition time t_t , the theoretical position errors e_{x-y} and e_z (20) of improved model (2) are constant. The theoretical position errors e_{x-y} and e_z are presented in Figure 2 for constant Mach number speed regime transition into the descent with a standard constant angle of $\theta = 3^\circ$.

While the horizontal plane e_{x-y} theoretical position error of improved model (2) is negligible, the vertical

plane e_z position error will be almost equal to the reduced vertical separation minimum (RVSM) standard in a high-speed long-duration transition into descent in the tail-wind conditions (Fig. 2).

3.2 Actual trajectory prediction errors

For absolute vertical plane trajectory prediction error determination the aircraft descent trajectories predicted for the next 900 seconds (15 minutes) using the simple (1) and improved (2) model of aircraft relative flight were compared with the actual flight data recorded on a commercial flight of Airbus A320 and Canadair CRJ200. The methodology used was chosen for its simplicity. The results of the descent trajectory prediction error determination are presented (as a single flight example) in Figure 3 while the test flight conditions data are provided in Tables 1 (test flight plan) and 2 (weather conditions).

From the aircraft trajectory generation point of view it was expected that the greatest inaccuracies of trajectory prediction will appear at the tropopause transition and while the aircraft descent speed regime is changed., In the stratosphere, namely, the aircraft true airspeed (TAS) is constant in the descent since the static air temperature (SAT) T is a constant, while in the troposphere it is a function of SAT as well as of aircraft speed regime defined either by constant Mach number M or the constant calibrated airspeed v_C . For descent trajectory segments of a special interest to be included, winter longer-range flights were chosen for the predicted trajectory accuracy investigation to assure that the top of descent is in the stratosphere (longer-range flights are flown higher for economy; in winter the tropopause is lower due to the lower-than-standard SAT at the ISA reference level). The Air Traffic Control imposed break in aircraft descent (between C and D in Figure 3) only fostered trustworthiness of a trajectory prediction error determination methodology.

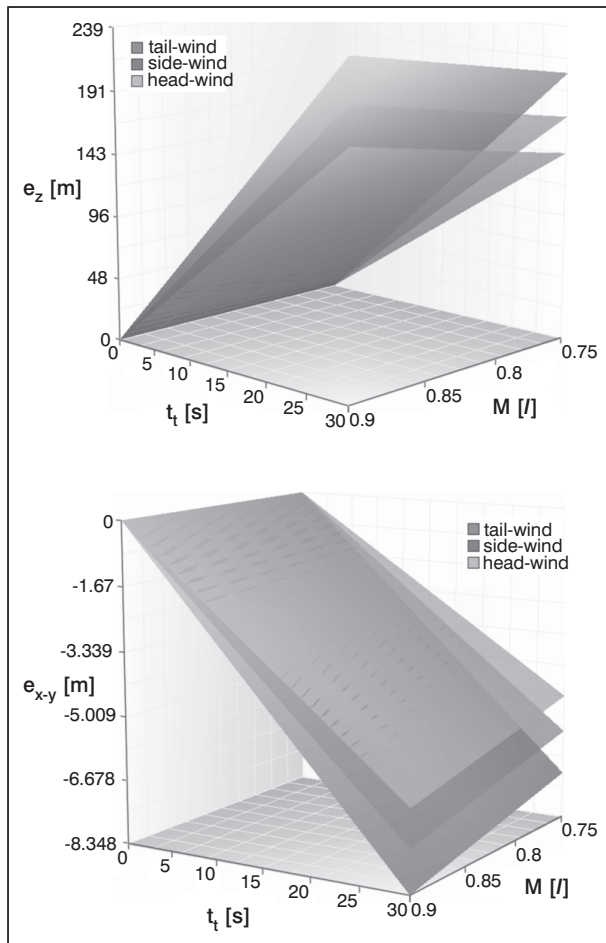


Figure 2 – The improved model aircraft position errors in vertical e_z and horizontal e_{x-y} plane after transition into descent.

Table 1 – Test flight plan (test example)

reference to Fig. 3	time		flight phase	planned flight parameters			
	of trajectory construction	of descent		Z	M	θ	v_C
	[s]			[m]	[/]	[°]	[kt]
	0		level cruise	11100	0.78	0	
A	132	$t_0 = 0$	descent				1.2
B	192.27	$t_{tp} = 60.27$ s	tropopause transit	10890			
C	338	$t_{CD1} = 206$ s	level cruise	10088		0	
D	431	$t_{CD2} = 299$ s	descent				
E	480.76	$t_p = 349.76$ s	descent & airspeed regime change	9410		3.2	280

Table 2 – Weather conditions report (test example)

time of trajectory construction	true heading	dynamic state of atmosphere ϑ_D		static state of atmosphere ϑ_S
	η	ξ	w	T_{0R}
[s]	[°]	[°]	[kt]	[K]
0	71	19	46	286.9
150	70	20		
300		17	49	
450	57	21	59	
600		17	61	
750		14	54	
900	48	12	49	

ISA-1.24 °C

The vertical plane trajectory prediction error e_{SIM} of a simple model of aircraft relative flight (1) clearly increases exponentially with the trajectory prediction look-ahead time (Figure 3). The reason for such rapid error increase is the fact that the simple model (1) is designed to be ignorant to the variation of an aircraft true airspeed (TAS, v) due to the static air temperature (SAT, T) gradient in the troposphere. Within next 300 seconds (5 minutes) after descent is resumed (E in Figure 3) the vertical plane trajectory prediction error of a simple model exceeds the RVSM standard by 30%. Consequently, the conflict detection based on the simple model of aircraft relative flight (1) will be unreliable or even impossible.

For the entire look-ahead time (15 minutes) of an aircraft future trajectory predicted with the improved model of flight (2) its vertical plane trajectory prediction error e_{IMP} is stable in oscillations within $\pm 16\%$ of the RVSM standard (Figure 3). Being for the factor of at least 3 more accurate in trajectory prediction as simple model (1), the improved model (2) promises greater reliability of conflict detection.

The general reason for the vertical plane trajectory prediction error e_{IMP} of improved model (2) oscillations between -50.4 m and $+69.6$ m are usual oscillations of actual flight speed parameters (Figure 3 below). The first abrupt amplitude in the e_{IMP} oscillation occurs (after D in Figure 3) due to the not-typical pilot imposed oscillation of the aircraft rate of descent when the descent resumed. The entire aircraft trajectory is predicted upon the reference SAT T below the aircraft at the beginning of its trajectory prediction ($t = 0$: Table 2, Appendix 2). Actual data documenting the SAT during test flight indicates the tropopause descent approximately 400 seconds from the start of trajectory prediction (an aircraft flew into the colder region) resulting in lower actual SAT than predicted. The actual aircraft TAS consequently decreased in the constant calibrated airspeed regime through the troposphere more slowly than predicted. That is why, with the increasing look-ahead time in the second half of the predicted trajectory, the oscillations of e_{IMP} continued.

The first abrupt amplitude in the e_{IMP} oscillation occurs (after D in Figure 3) due to the not-typical pilot imposed oscillation of the aircraft rate of descent when the descent resumed. The entire aircraft trajectory is predicted upon the reference SAT T below the aircraft at the beginning of its trajectory prediction ($t = 0$: Table 2, Appendix 2). Actual data documenting the SAT during test flight indicates the tropopause descent approximately 400 seconds from the start of trajectory prediction (an aircraft flew into the colder region) resulting in lower actual SAT than predicted. The actual aircraft TAS consequently decreased in the constant calibrated airspeed regime through the troposphere more slowly than predicted. That is why, with the increasing look-ahead time in the second half of the predicted trajectory, the oscillations of e_{IMP} continued.

3.3 Trajectory prediction accuracy improvements

The improved model of aircraft relative flight (2) accuracy level depends on the future static

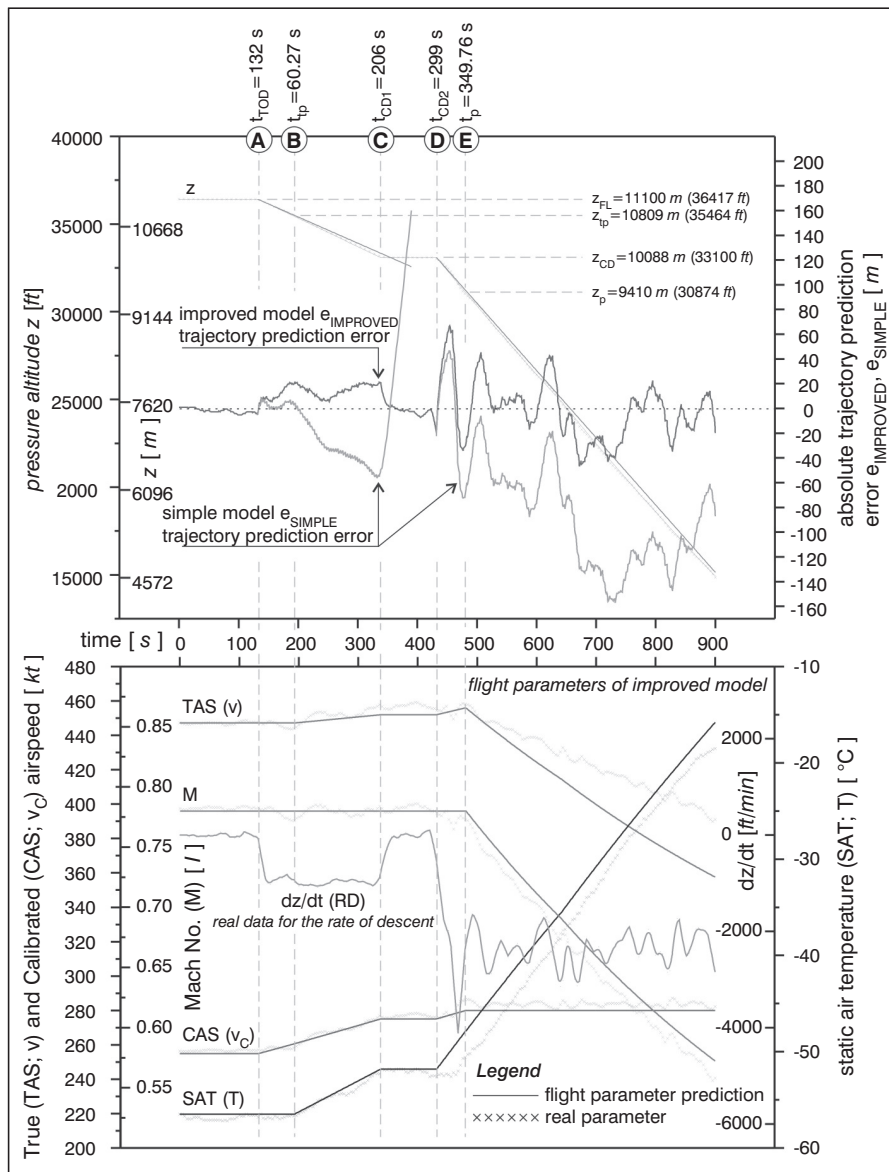


Figure 3 – Vertical plane trajectory prediction error of a simple and improved model of aircraft relative flight

$\vartheta_S(z) = \{T(z)\}$ and dynamic $\vartheta_D(z) = \{w(z), \xi(z)\}$ state of atmosphere prediction availability. The aircraft TAS is sensitive to the future SAT T prediction especially in the troposphere and the aircraft relative (ground) speed in consecutive to the wind speed w and direction ξ predictions.

The accuracy of four-dimensional airborne traffic situation prediction can be augmented if ASAS on-board each aircraft is provided via data-link with the detailed atmospheric conditions in the format proposed in Figure 4. The static state of atmosphere $\vartheta_S = \{\Delta T(x, y)\}$ should include the data about the SAT difference ΔT between the standard and the real atmosphere reference SAT at reference pressure altitude $z(p_0)$ for a grid of nodes defined by their longitude x and latitude y ; the dynamic state of atmosphere $\vartheta_D = \{w(x, y, z(p)), \xi(x, y, z(p))\}$ should be format-

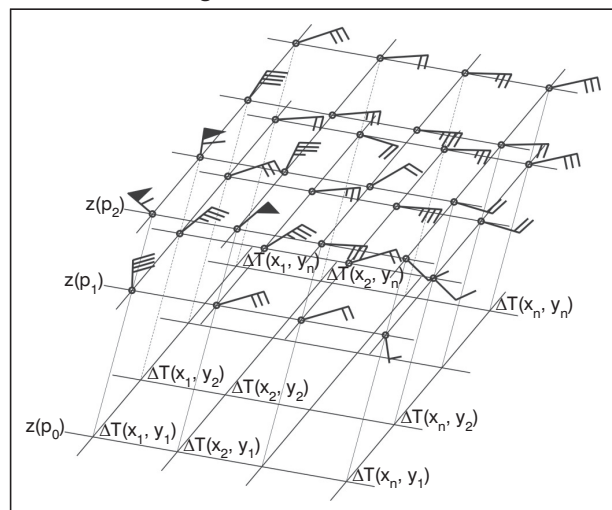


Figure 4 – Proposed atmospheric conditions data format

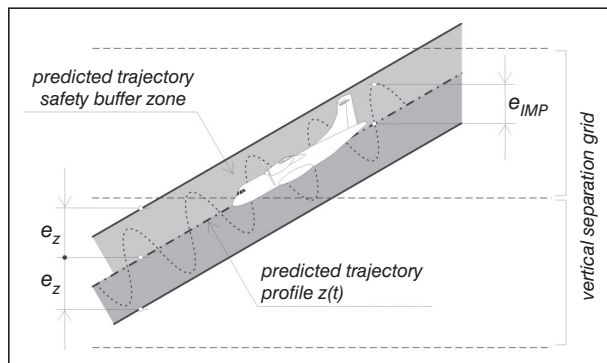


Figure 5 – Predicted aircraft trajectory with vertical safety buffer

ted three-dimensionally with the horizontal plane defined by x and y while the vertical plane is defined by the pressure altitude $z(p)$.

The aircraft trajectory prediction error analysis revealed that the vertical plane trajectory prediction error of model (2) is even for longer prediction periods with the same parameters of flight smaller than the theoretical vertical plane position error $e_{IMP} < e_z$. The latter is thus useful for the construction of a safe buffer zone extending in the vertical plane for the value of e_z on either side of the predicted aircraft trajectory $z(t) - e_z \leq z(t) \leq z(t) + e_z$ as presented in Figure 5, since the theoretical vertical position error is constant after transition time $t \geq t_t$.

5. CONCLUSION

The airborne dependant surveillance-broadcast (ADS-B) system based and cockpit display of traffic information (CDTI) compatible model of aircraft relative flight (2) can predict aircraft trajectory for up to 15 minutes in advance with limited and not-exciting position prediction error, and therefore enabling stable prediction of long-range future four-dimensional airborne traffic situation. Accordingly, the comparison revealed that the improved model (2) outperforms its TCAS-type simple model (1) pendant in terms of trajectory prediction accuracy promising better conflict detection accuracy and reliability. Especially distinctive are its performances at trajectory predictions for climbing and/or descending flights through the troposphere where the characteristic temperature gradients affect the aircraft speed parameters. The attribute of improved model preference is the feasibility of its trajectory prediction accuracy improvement providing it with detailed atmospheric conditions data.

ACKNOWLEDGEMENTS

This material is based on the work supported by the Slovenian Research Agency Target Research Program – Science for Peace and Security under Grant No.: M2-0118.

The author is sincerely grateful to Cpt. Aleksander Sekirnik of Adria Airways for his unselfish support, advice, and help.

Dr. TONE MAGISTER

E-mail: tone.magister@fpp.edu

Univerza v Ljubljani, Fakulteta za pomorstvo in promet
Pot pomorščakov 4, 6320 Portorož, Republika Slovenija

POVZETEK

NAPAKE POLOŽAJA PREDVIDENE PRIHODNJE TRAJEKTORIJE LETALA

Članek obravnava izboljšanje natančnosti načrtovanja prihodnje trajektorije letala za zagotavljanje razdvajanja letal v zraku na daljših razdaljah. Strateško načrtovanje varnih letov in učinkovita taktika izogibanja nevarnostnim stanjem v zraku narekuje pravočasno in pravilno zaznavanje nevarnostnih stanj, ta temelji na predvideni prihodnji štiri-dimenzionalni prometni situaciji v zraku, katere natančnost je tolikšna, kolikšna je natančnost, s katero je predvidena prihodnja trajektorije vsakega letala. Študija je osredotočena na razvoj izpopolnjene kinematičnega modela relativnega leta letal in na njegovo natančnost določanja položaja letala v zraku. Operativne sposobnosti za vzpostavljjanje in ohranjanje razdvajanja letal v zraku so opisane na osnovi primerjave izpopolnjene in preproste modela relativnega leta letal.

KLJUČNE BESEDE

predvidena trajektorija leta letala, napaka predvidene trajektorije leta, napaka predvidenega položaja letala, varnost letenja

LITERATURE

- [1] Duong, V., Gawinowski, G., Nicolaon, J.-P., Smith, D., Sector-Less Air Traffic Management, 4th USA/Europe ATM R&D Conf., Santa Fe, USA, 2001
- [2] Brooker, P.: Airborne Separation Assurance Systems: towards a work programme to prove safety, Safety Science, No. 42, 2004, pp. 723-754
- [3] Erzberger, H., The Automated Airspace Concept, 4th USA/Europe ATM R&D Conf., Santa Fe, NM, USA, 2001
- [4] Filippone, A.: Comprehensive analysis of transport aircraft performance, Progress in Aerospace Sciences, No. 44, 2008, pp. 192-236
- [5] Hoekstra, J. M.: Designing for Safety – The Free Flight Air Traffic Management Concept, Ph. D. thesis, Technische Universiteit, Delft, The Netherlands, 2001
- [6] Hoekstra, J. M., van Gent, R. N. H. W., Ruigrok, R. C. J.: Designing for safety: the “free flight” air traffic manage-

- ment concept, Reliability Engineering and System Safety, No. 75, 2002, pp. 215-232
- [7] **Loft, S., Bolland, S., Humphreys, M. S., Neal, A.:** *A Theory and Model of Conflict Detection in Air Traffic Control*, Journal of Experimental Psychology: Applied, Vol. 15, No. 2, 2009, pp. 106-124
- [8] **Magister, T.:** *Transition flight between the autonomous flight airspace and automated airspace*, PROMET-Traffic&Transportation, Vol. 20, No. 4, 2008, pp. 215-221
- [9] **Tomlin, C.:** *Hybrid Control of Air Traffic Management Systems*, Ph. D. thesis, University of California at Berkeley, USA, 1998
- [10] **Wangermann, J. P., Stengel, R.:** *Principled negotiation between intelligent agents: a model for air traffic management*, Artificial Intelligence in Engineering, No. 12, 1998, pp. 177-187
- [11] **Weigang, L., de Souza, B. B., Crespo, A. M. F., Alves, D. P.:** *Decision support system in tactical air traffic flow management for air traffic flow controllers*, Journal of Air Transport Management, Vol. 14, No. 6, 2008, pp. 329-336